Chemical Physics Letters 738 (2020) 136868

Contents lists available at ScienceDirect

Chemical Physics Letters

journal homepage: www.elsevier.com/locate/cplett

Research paper

Spectroscopy and crystal chemical properties of $NaCa_2[Si_4O_{10}]F$ natural agrellite with tubular structure

Kaneva Ekaterina[a,b,*], Shendrik Roman[a], Mesto Ernesto[c], Bogdanov Aleksandr[a], Vladykin Nakolay[a]

[a] Vinogradov Institute of Geochemistry, Siberian Branch of the Russian Academy of Sciences, 1A Favorsky Str., 664033 Irkutsk, Russia
[b] Irkutsk National Research Technical University, 83 Lermontov Str., 664074 Irkutsk, Russia
[c] University of Bari "Aldo Moro", Dip. di Scienze della Terra e Geoambientali, 4 Orabona Str., 70125 Bari, Italy

HIGHLIGHTS

- The simplified formula of the investigated agrellite samples is $NaCa_2[Si_4O_{10}]F$.
- Crystal structure corresponds to the model of REE-agrellite.
- Manganese ion is incorporated at Ca sites, surrounded by two fluorine ions.
- Luminescence due to 5d-4f transition in Ce^{3+} ions was observed.
- Materials based on RE-doped agrellite can be considered as promising phosphors.

ARTICLE INFO

Keywords:
Inosilicate
Tubular structure
Agrellite
Spectroscopy
Luminescence
Crystal chemistry

ABSTRACT

Agrellite is a rare inosilicate, having a crystal structure characterized by SiO_4-tetrahedral tubes located between continuous wall layers formed by edge-sharing Ca-polyhedra. A detailed crystal chemical and physical study of agrellite specimens is carried out by means of electron probe microanalysis, Fourier transform infrared spectroscopy, electron-paramagnetic resonance, and single crystal X-ray diffraction. Additionally, the electronic structures of agrellite was calculated. Luminescence due to 5*d*-4*f* transition in Ce^{3+} ions is observed in both investigated samples. EPR analysis points out the Mn^{2+} replaces Ca^{2+} ion in Ca(1A) and Ca(2B) positions, coordinated by two F sites.

1. Introduction

Nanostructured inorganic, organic and biological materials have existed in nature since the evolution of life on Earth. Modern science pays great attention to the creation of new materials, functional structures and devices on a nanometer scale. At the same time, interest in tubular molecular structures is associated with the development of nanoscience. Currently, SiO_2-based nanotubes are synthesized, many studies are devoted to modeling silicon-oxygen nanostructures based on topological analogy of the structures of carbon and silicate complexes. In this regard, the study of natural phases, which have tubular fragments in their structure, plays an important role. This type of compound includes natural inosilicate agrellite.

For the first time, agrellite was found as rock-forming mineral in regional metamorphic alkaline rocks of Kipawa alkaline complex, Quebec province (Canada) [1]. The symmetry was established as triclinic, sp. gr. $P\bar{1}$. The crystal structure has been solved in 1979 by [2].

In 1998 [3,4] reported X-ray powder diffraction data and single crystal X-ray investigation of a strontium agrellite from Yakutian charoitites, Murun massif. A difference in arrangement of silicate-sodium layers in the crystal structures of russian and canadian agrellite was registered. The russian [4,5] and canadian [1,2] agrellites also differ in their chemical composition, but they have close unit-cell parameters. Calcium atoms in agrellite from the Murun massif, Russia, are partially replaced by strontium. In agrellite from Quebec, Canada, rare earth elements substitute Ca. The simplified formulas are: $Na(Ca_{1.75}Sr_{0.16})[Si_4O_{10}](F,(OH))$ [4] and $Na(Ca_{1.91}REE_{0.10})[Si_4O_{10}]F$ [2], respectively.

In the present work, a detailed chemical, physical and structural study is carried out for the first time on agrellite specimen from the

* Corresponding author at: Vinogradov Institute of Geochemistry, Siberian Branch of the Russian Academy of Sciences, 1A Favorsky Str., 664033 Irkutsk, Russia.
E-mail address: kev604@mail.ru (E. Kaneva).

https://doi.org/10.1016/j.cplett.2019.136868
Received 19 July 2019; Received in revised form 29 August 2019; Accepted 15 October 2019
Available online 17 October 2019
0009-2614/

Dara-i-Pioz massif. The results are compared with the data obtained for the agrellite from the Murun massif.

2. Materials and methods

2.1. Samples description

The studied agrellite was taken from two complexes of alkaline rocks: Dara-i-Pioz (Tajikistan) and Murun (Russia) massifs. The Dara-i-Pioz massif is located in the southwest Tien Shan Mountains close to the Pamirs in Tadjikistan. The Murun alkaline complex is the southwest edge of the Aldan shield, located directly on border of Yakutia and the Irkutsk region (Russia). Agrellites form large elongated greyish-white crystals up to 5 cm in size. The samples fluoresce bright pink under photo and X-ray excitation in UV.

2.2. Chemical analysis

Electron probe microanalysis was performed on two single crystals of Dara-i-Pioz agrellite (hereafter agr_dp) and two single crystals of Murun agrellite (hereafter agr_mur), embedded in epoxy resin, polished and then carbon coated. A JEOL JXA-8200 electron probe micro-analyzer operating at accelerating voltage of 15 kV and a beam current of 5 nA was used (spot size ~ 1 μm and counting time – 40 s). Full wavelength dispersive spectrometry (WDS) mode was employed. A Phi-Rho-Z routine was employed for the conversion from X-ray counts to oxide weight percentages (wt%).

2.3. Single crystal X-ray diffraction study

Single crystal X-ray diffraction (SCXRD) data were collected from crystals, selected by hand picking at the binocular microscope, at room temperature using Bruker-AXS X8 APEXII automated diffractometer equipped with a four-circle Kappa goniometer, CCD detector with a maximum active area diameter of 90 mm and a monochromatized MoKα radiation (operating conditions – 50 kV and 30 mA, crystal-to-detector distance – 40 mm).

The collection strategies were optimized by the COSMO program in the APEX2 suite package [6] and the entire Ewald sphere (± h, ± k, ± l) up to $\theta_{max} \sim 40^\circ$ was recorded by a combination of several ω and ϕ rotation sets, with 0.5° scan width and 10–60 s per frame exposure time. Reflection intensities were extracted and corrected for Lorentz-polarization using the SAINT package [7]. A semi-empirical absorption correction was applied by means of the SADABS software [8]. The XPREP software assisted in the determination of the space group and in the calculation of the intensity statistics. Finally, least-squares refinements were performed using the program CRYSTALS [9]. The crystal structure was verified with the use of the charge flipping algorithm [10]. The space group ($P\bar{1}$) and the atomic positions were confirmed by the analysis of the reconstructed electronic density. Reflections with $I > 3\sigma(I)$ were considered as observed and the refined parameters were: scale factor, atomic positions, and anisotropic atomic thermal displacement parameters. In the anisotropic refinements, the R values for the compound dropped to R = 6.0–15.8% and R = 3.4–5.6% for agrellite samples from Dara-i-Pioz and Murun massif, respectively. The unit cell parameters of studied samples are given in Table 1. The results and some details of data collection and structure refinements, atom coordinates and selected interatomic distances are available from the authors.

2.4. Spectroscopy study

The Fourier Transform Infrared (FTIR) measurements were carried out using a Simex FT-801 spectrometer. Agrellite powder in a dehydrated KBr pellet (600 °C, 30 min) was subsequently heated over the temperature range from 25 to 530 °C at 50 °C intervals. Then the powder was pressed onto wafer (thick – 0.04 mm, diameter – 4 mm). The absorption spectra were measured concerning KBr powder wafer without agrellite heated at the same temperature. Infrared spectra were acquired from 4000 to 450 cm^{-1}.

The diffusion optical absorption spectra were obtained by a Perkin-Elmer Lambda 950 UV/VIS/NIR spectrophotometer at 300 K using an integrated sphere as proposed in [11]. The photoluminescence spectra were recorded with a MDR2 grating monochromator, a photomodule Hamamatsu H6780-04 (185–850 nm) photon-counter unit and a Perkin Elmer LS-55 spectrometer. The luminescence spectra were corrected for

Table 1
Lattice parameters and average chemical composition (wt%) of the studied Dara-i-Pioz and Murun agrellite and crystal chemical formulas of the studied and literature agrellite.

	Dara-i-Pioz massif (Tajikistan)		Murun massif (Russia)		
	agr_dp_1	agr_dp_2	agr_mur_1	agr_mur_2	
Lattice parameters	a = 7.7550(5), b = 18.938(1), c = 6.9826(4) Å, α = 89.706(4), β = 116.611(4), γ = 94.393(5)°, V = 913.7(1) Å^3		a = 7.7628(1), b = 18.9505(4), c = 6.9847(1) Å, α = 89.774(1), β = 116.581(1), γ = 94.311(1)°, V = 915.80(3) Å^3		
					Used standards
SiO_2	60.9(7)	60.4(6)	60.2(7)	60.5(8)	Wollastonite
Na_2O	7.9(2)	7.6(2)	7.9 (2)	7.6(9)	Omphacite
MgO	0.03(1)	0.04(2)	0.02(1)	0.04(2)	Olivine
K_2O	0.13(2)	0.12(3)	0.17(3)	0.4(2)	K-felspar
CaO	27.4(2)	27.5(3)	27.1(5)	27.1(8)	Anorthite
MnO	0.13(4)	0.16(3)	0.08(4)	0.09(5)	Rhodonite
FeO	0.15(4)	0.17(6)	0.06(4)	0.08(2)	Fayalite
SrO	0.1(2)	0.1(2)	0.9(1)	0.9(2)	Celestine
ZrO_2	0.1(3)	b.d.l.	b.d.l.	0.1(2)	Zr-jarosite
BaO	0.09(9)	0.08(9)	b.d.l.	b.d.l.	Sanbornite
Ce_2O_3	0.13(6)	0.14(8)	0.1(1)	0.14(8)	Ce-phosphate
F	4.8(1)	4.7(7)	4.5(3)	4.5(6)	F-horneblende
	101.86	101.01	101.03	101.45	
O = F	2.02	1.98	1.89	1.89	
Sum	99.84	99.03	99.14	99.56	

b.d.l. = below detection limit
Al_2O_3, TiO_2, ZnO, Cs_2O, CuO, Y_2O_3, Nb_2O_5, La_2O_3, Pr_2O_3, Nd_2O_3, Sm_2O_3, Eu_2O_3, Gd_2O_3, Dy_2O_3, Ho_2O_3, Er_2O_3, Yb_2O_3, Lu_2O_3, HfO_2 – b.d.l.

Source	Crystal chemical formula
[1] Quebec, Canada	$(Na_{1.01}K_{0.02})(Ca_{1.82}REE_{0.12}M_{0.04})$ $Si_{3.90}Al_{0.01}O_{9.92}(F_{0.93}(OH)_{0.18})$ *Simplified*: $Na(Ca_{1.82}REE_{0.12})[Si_4O_{10}](F,(OH))$
[2] Quebec, Canada	*Simplified*: $Na(Ca_{1.91}REE_{0.10})[Si_4O_{10}]F$
[5] Murun, Russia	$(Na_{1.00}K_{0.01})(Ca_{1.75}Sr_{0.18}Mn_{0.02})[Si_{4.03}O_{10}]$ $(F_{0.58}(OH)_{0.42})\cdot 0.2H_2O$ $(Na_{1.02}K_{0.01})(Ca_{1.59}Sr_{0.33}Ce_{0.01}La_{0.01})[Si_{4.03}O_{10}]$ $(F_{0.62}(OH)_{0.38})$ $(Na_{1.03}K_{0.01})(Ca_{1.47}Sr_{0.46}Ce_{0.01}La_{0.01})[Si_{4.02}O_{10}]$ $(F_{0.73}(OH)_{0.27})$ *Simplified*: $Na(Ca_{1.75}Sr_{0.18})[Si_4O_{10}](F,(OH))$
[4] Murun, Russia	$(Na_{0.94}K_{0.03})(Ca_{1.75}Sr_{0.16})[Si_4O_{10}]$ $(F_{0.78}(O,OH)_{0.22})\cdot 0.24H_2O$ *Simplified*: $Na(Ca_{1.75}Sr_{0.16})[Si_4O_{10}](F,(OH))$
This study, Dara-i-Pioz, Tajikistan	agr_dp_1: $(Na_{0.99}K_{0.01})(Ca_{1.95}Na_{0.03}Mn_{0.01}Fe_{0.01})$ $[Si_4O_{10}]F$ agr_dp_2: $(Na_{0.99}K_{0.01})(Ca_{1.98}Mn_{0.01}Fe_{0.01})[Si_4O_{10}]F$ *Simplified*: $NaCa_2[Si_4O_{10}]F$
This study, Murun, Russia	agr_mur_1: $(Na_{0.99}K_{0.01})(Ca_{1.94}Sr_{0.03}Na_{0.02}(Mn,Fe)_{0.01})$ $[Si_4O_{10}](F_{0.96}OH_{0.04})$ agr_mur_2: $(Na_{0.97}K_{0.03})(Ca_{1.94}Sr_{0.03}Na_{0.02}(Mn,Fe)_{0.01})$ $[Si_4O_{10}](F_{0.95}OH_{0.05})$ *Simplified*: $NaCa_2[Si_4O_{10}]F$

spectral response of detection channel. The photoluminescence excitation (PLE) spectra were measured with Perkin-Elmer LS-55 for direct 4f-5d excitation and vacuum monochromator VM-2 (LOMO) and Hamamatsu deuterium lamp L7292 for measurements in VUV spectral region. The PLE spectra were corrected for the varying intensity of exciting light due. The X-ray excited luminescence was performed using an X-ray tube operating at 50 kV and 1 mA.

The Electron Paramagnetic Resonance (EPR) experiments of agrellite single crystals were performed on an X-band spectrometer (RE-1306) operating at a microwave frequency in the vicinity of 9380 MHz in connection with a cryostat suitable for temperatures of 77 and 295 K.

3. Results and discussion

3.1. Chemical composition

The average compositions (determined over five-eight spots) are reported in Table 1. The formulas of the investigated samples were calculated on the basis of 4 silicon atoms per formula unit (apfu) and are also given in Table 1. Agrellite of the present work are compared with the literature data. Note that the amount of Sr is lower and Fe and Mn contents are higher in Dara-i-Pioz agrellite compared to that from Murun.

According to the obtained data, the simplified formula of studied agrellites is $NaCa_2[Si_4O_{10}]F$, the REEs and Sr are present in the structure in minor amounts (≤ 0.04 apfu). Therefore, one cannot to rank the mineral as one of the previosly described varieties – REE-agrellite [1,2] or Sr-agrellite [3–5].

3.2. Structural description

Agrellite belongs to a special group of silicates – inosilicates. The crystal structure is characterized by the presence of silicate tubes, represented by loop-branched dreier double chain having the following description: $\{1B, 2^1_\infty\}[^3Si_8O_{20}]$ [12]. The silicate tube consists of two centrosymmetrically-related single silicate chains. Each single chain is formed by corner-sharing four-membered tetrahedral rings, the same as the $[Si_4O_{11}]$ vlasovite chain [13]. These rings are concatenated into chains along the *c* axis trough the vertex. Two neighboring centrosymmetrically related vlasovite chains are linked by oxygen, resulting in a silicate tube with the composition $[Si_8O_{20}]$. Its diameter is defined by a basket-shaped six-membered ring. Each tube contains two different eight-membered tetrahedral rings, which have four tetrahedra in common. The ring is joined to Ca polyhedra. The studied agrellite crystal structure is depicted in Fig. 1.

There are two crystallographically distinct silicate tubes (*A* and *B*), running parallel to *c*, their configurations are only slightly different from each other. The isolated silicate tubes are linked with the building layers of the edge-shared Ca-polyhedra (Ca(1A), Ca(1B), Ca(2A) and Ca (2B)). The Na(A) and Na(B) atoms are located in eight-membered rings.

The comparison between crystal structures of Sr-agrellite from Russia and REE-containing agrellite from Canada revealed differences in relative position of the silicate tunnel layers and the related sodium cations, indicating the manifestation of polytypism phenomena in this mineral [4,14]. With the same position of the calcium layers, the polytypes differ by a shift of one silicate layer relative to another one by about 1/2 translation along the *c* axis. The canadian (REE-agrellite) and yakutian (Sr-agrellite) minerals are referred to, respectively, as agrellite-$2A_c$ and agrellite-$2A_I$ [3,4].

Crystal structure of investigated samples corresponds to the model proposed by [2]. The mutual arrangement of the *A* and *B* silicate tubes conforms to that of REE-agrellite.

The sodium atoms are located within the voids formed by the eight-membered silicate rings. [4] reported that Na are located in the octahedra, while Na-polyhedra in REE-agrellite were described as distorted cubes [2]. In agrellite from Dara-i-Pioz and Murun massifs, the Na

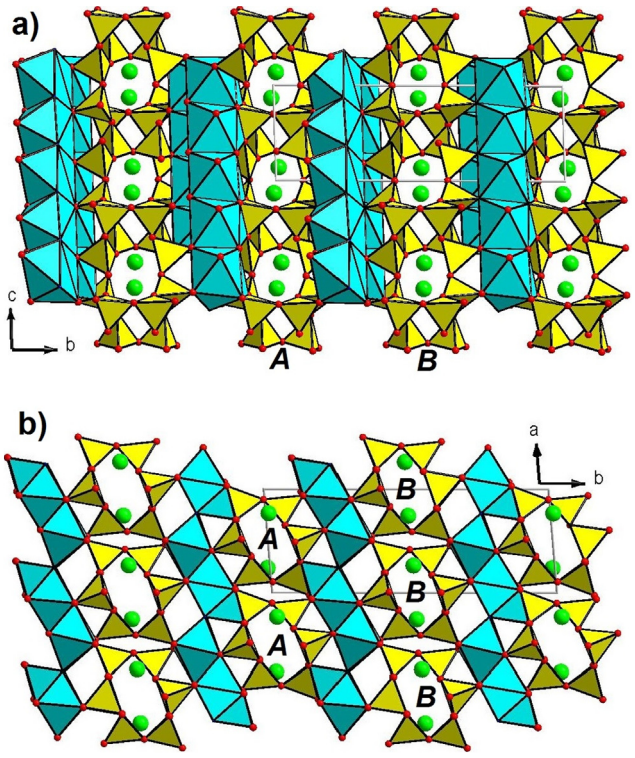

Fig. 1. Perspective views of agrellite crystal structure projected down to (a) *a* axis and (b) *c* axis. SiO_4 tetrahedra and Ca-polyhedra are drawn in yellow and cyan, respectively; sodium atoms are drawn in green. Unit cell edges and *A* and *B* tubes are designated. (For interpretation of the references to color in this figure legend, the reader is referred to the web version of this article.)

atoms are eight-fold coordinated. Each sodium polyhedron shares six vertexes with the silicate tube below and another two with the tube above.

Oxygen atoms of the silicate tubes and F atoms are positioned on the vertices of the calcium polyhedra. Authors [4] reported that Ca(1A) and Ca(2B) atoms locate in seven-vertex polyhedra, while Ca(2A) and Ca (1B) are octahedrally coordinated. According to [2] the Ca(1A) and Ca (2B) are [8]-coordinated irregular polyhedra, surrounded by six O and two F atoms, while the Ca(2A) and Ca(1B) are octahedrally coordinated by O atoms. All isomorphic substitutions, to a greater degree calcium for strontium or rare earth elements, occur precisely in the Ca(1A) and Ca(2B) positions [2,4]. In the studied agrellites, the coordination number of Ca-atoms correspond to the data reported for REE-agrellite and the ⟨Ca-O⟩ and ⟨Ca-F⟩ values are close to average distances obtained by [2].

The electronic structures of pure and Eu^{2+} containing agrellite were calculated within density functional theory framework with PBEsol [15] exchange-correlation functional, as implemented in the VASP [VASP-citation] code. First, the positions of all atoms were optimized while lattice vectors were kept fixed at their experimental values. Then, the electronic structure was calculated. The threshold imposed on cartesian components of forces during geometry optimization was 0.01 eV/A, and the total energy of relaxed structure was converged to 1.0E−7 eV. For Eu^{2+} containing agrellite one Ca atom in the unit cell was replaced by Eu one. The total spin imposed on the Eu-containing system was 7/2, as Eu^{2+} has seven unpaired electrons on its f-shell.

Fig. 2a (dos_pure) represents density of electronic states in pure agrellite. The very top states of the VB are formed by oxygen p-states while slightly deeper the p-states of fluorine are found. The bottom of conduction band is formed by d-states of calcium. The bonding in agrellite possess covalent nature: p-orbitals forming top of the VB are overlapping with empty Ca d-states.

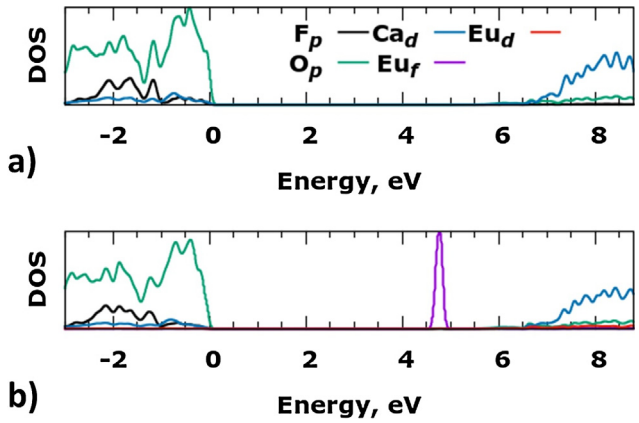

Fig. 2. Density of electronic states in agrellite: (a) pure agrellite; (b) Eu^{2+} containing agrellite [2]

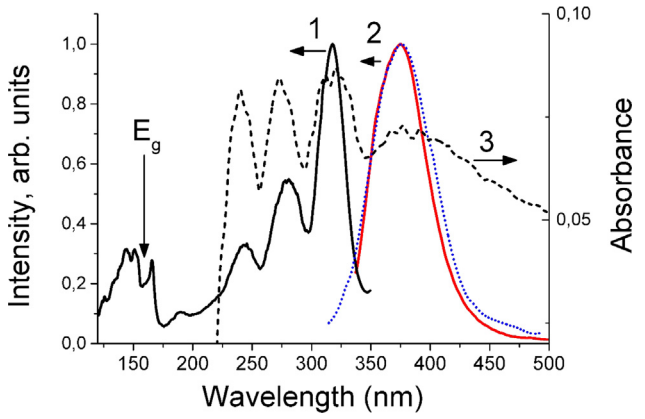

Fig. 3. Excitation (solid curve 1), photoluminescence (solid red curve 2), X-ray excited luminescence (dashed curve 3) and diffuse optical absorption spectra (dotted blue curve) of agrellite sample from Dara-i-Pioz massif. (For interpretation of the references to color in this figure legend, the reader is referred to the web version of this article.)

A calculation of Eu^{2+} containing agrellite (from [2]) was made in order to estimate the possibility of luminescence of divalent RE-ions. In this case the Eu^{2+} f-states appear closer to the bottom of CB than to the top of VB which pushes the d-states of europium even higher to the conduction band (Fig. 2b dos_Eu). Under these circumstances, and assuming that the Eu^{2+} electronic structure is associated with the deepest location of the f-shell among all divalent RE-elements, we conclude that the other RE-elements in divalent state would have their d-levels even higher in the CB which would eliminate the luminescence of the divalent REE in agrellite. However, for trivalent case, the 4f states of RE-elements would be locate deeper in the band gap, therefore, a 5d–4f luminescence would be possible which is consistent with experiments.

3.3. Spectroscopic data

The infrared spectra of agrellite samples are given in Fig. S1a, b, available as Supplementary Information. The group of peaks observed at 1136, 1093, 1061, 1041, 1003, 959 cm^{-1} (Fig. S1a) may be assigned to the asymmetric Si—O stretching modes of the SiO_4 tetrahedra, while the sharp peaks in mid-frequency range at about 709, 687, 652, 610 cm^{-1} can be attributed to the Si—O—Si bending mode as well as the symmetric O—Si—O stretching vibrations [16]. The peaks at about 585 and 777 cm^{-1} may be assigned to the symmetric Si—O and O—SiO vibration, respectively [1]. Similar band structure was given for agrellite by [17]. The peak at about 535 cm^{-1} can correspond to the stretching of Ca—O. The broad peak at about 1417 cm^{-1} observed in Murun sample may be attributed to carbonate impurity. The higher frequency part of the peak can be due to water bending modes.

In Murun sample the strong wide bands in 2800–3700 cm^{-1} spectral region (Fig. S1b) correspond to the symmetric and asymmetric stretching vibration of the H_2O. The sharp peak at about 3555 cm^{-1} can be ascribed to the stretching modes of OH^- ions. The frequency of the vibration is close to the free OH^- anion (3555.6 cm^{-1}). In Darai-Pioz sample absorption spectrum the wide band in region of 2700–3700 cm^{-1} is absent and the weak sharp peak at about 3555 cm^{-1} is observed.

In Fig. S2, available as Supplementary Information, thermal dehydroxylation curves of Murun sample measured at 3555 cm^{-1} (OH^-) and 3155 cm^{-1} (H_2O) bands are given. This figure shows the relative intensities of the hydroxyl and H_2O bands in samples quenched over the temperature range from 25 to 530 °C at 50 °C intervals. The diagram clearly shows the dehydroxylation mostly taking place over 200–380 °C temperature range. However, OH^- absorption disappears completely at a 530 °C.

Since water molecules were not localized by the crystal structure refinement, the detected water is not structural. Taking into account the rather high temperature of water release when heated, it can be assumed that water has a zeolitic character and locates in the voids of the silicate tubes, not having a specific structural position.

3.4. Luminescence of Ce^{3+} ions

Agrellite samples demonstrate luminescence under photo and X-ray excitation in near UV region. Photoluminescence under 317 nm excitation and X-ray excited luminescence spectra are given in Fig. 3, curves 2 and 3, respectively. In the spectra wide band peaked at about 370 nm is observed. Excitation spectrum monitored at 370 nm is given in curve 1. In the spectrum 5 bands peaked at 190, 220, 245, 281, 317 nm appear. The similar bands are found in diffuse optical absorption spectrum (dashed curve in Fig. 3). The luminescence band is related to 5d-4f transition in Ce^{3+} ions in Ca^{2+} position. Five peaks in excitation spectrum correspond to transitions from ground 4f state of Ce^{3+} ion to crystal field splitted 5d state. Ce^{3+} ions has low symmetry point group, therefore, 5d state is splitted into 5 levels [18].

In excitation spectrum in VUV region narrow peaks in spectral region 120–170 nm are observed. These peaks is attributed to interband transition between top of valence band and bottom of conduction band. Assuming that peak at about 167 nm is due to first exciton transition band gap could be estimated using method given in [19] and [20]. The band gap is about 8 eV. The band gap value is typically for silicate media where top of valence band is formed by filled electronic states of oxygen ions and bottom of conduction band is formed by free electronic states of silicon ions.

Using the 5d levels energy measured from excitation spectrum in Fig. 4 the position of ground and excited states of all trivalent and divalent lanthanides in relation to vacuum energy can be calculated using VRBE model promoted by P. Dorenbos [20]. According to the diagram, wavelength of absorption band attributed to Ce^{4+} charge transfer can be estimated [21]. There is at about 400 nm. In absorption spectrum of agrellite given in Fig. 3 the similar wide band at about 390 nm is observed. Therefore, gray color of the sample is due to the Ce^{4+} charge transfer band.

From the diagram, it is clearly seen that ground states of divalent lanthanides are located close to the bottom of conduction band. Therefore, one could not expect a luminescence of divalent lanthanides in agrellite. However, trivalent Eu, Tb, Pr, Nd, Dy ions can demonstrate bright 4f-4f luminescence. Therefore, materials based on agrellite doped with rare earth ions can be considered as promising phosphors.

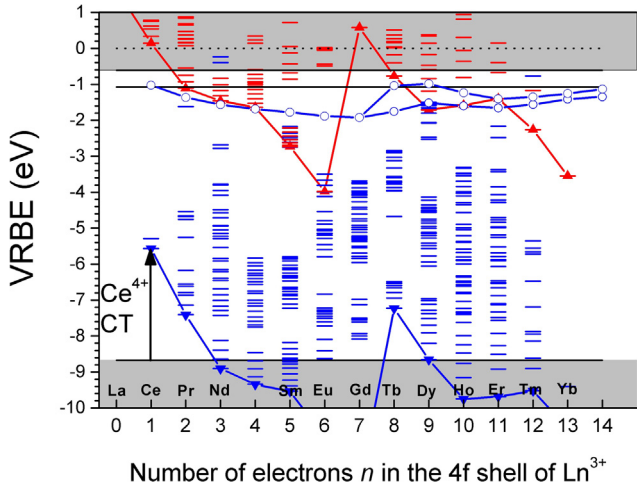

Fig. 4. The diagram shows the vacuum referred binding energies (VRBE) for electrons of divalent (red) and trivalent (blue) lanthanide ions with respect to the vacuum level of agrellite from Dara-i-Pioz massif. The zigzag red curve with triangles connects the $4f^n$ ground state energies of the divalent lanthanide ions. Blue zigzag curve with triangles respects to $4f^n$ ground state energies of trivalent lanthanide ions and blue curve with circles are their – $4f^{n-1}$ $5d^1$ states. (For interpretation of the references to color in this figure legend, the reader is referred to the web version of this article.)

3.5. Electron-paramagnetic resonance

In agrellite samples, EPR signal at room and 77 K temperatures was observed. The EPR spectra measured at 77 K along different crystallographic directions are given in Fig. 5. The EPR spectra contain well-resolved sextet structure with 90 Gauss splitting with g-factor of 2.001. The intensities of all bands are equal and they are attributed to Mn^{2+} ions (I = 5/2). Manganese can be normally substitutionally incorporated into agrellite crystal structure at a cation calcium site and surrounded by two fluorine ions. Thus, these are the Ca(1A) and Ca(2B) structural positions. All bands demonstrate additional structure due to superhyperfine interaction of the unpaired electron with two equivalent fluorine nuclei at angle 90°. For the simulations of the EPR spectra Easyspin Matlab package [22] was used. Calculated spectra along different direction of magnetic field are shown in Fig. 5 (green curves). All hyperfine and superhyperfine structure lines are in good coincidence with the experimental curves. Mn^{2+} ion with d^5 configuration can be exist in two possible spin states, the high spin state with S = 5/2 and low-spin state with S = 1/2. We simulated the both spin states in agrellite structure. EPR spectrum of an electron (S = 1/2, g = 2.001) with the hyperfine interaction of the Mn^{2+} ($A(Mn)$ = 265 MHz, I (Mn) = 5/2) and superhyperfine interaction with two equivalent fluorine nuclei ($I(^{19}F)$ = 1/2, A_1 = 41 MHz, A_2 = 59 MHz, A_1 = 10 MHz) could be described with the following spin-hamiltonian:

$$H = \beta gSB + A(Mn)SI(Mn) + 2A_1S_1I_1 + A_2S_2I_2 + A_3S_3I_3$$

where β is the Bohr magneton $A(Mn)$ and $A_{1\text{-}3}(^{19}F)$ are effective HF (SHF) constants of the Mn and ^{19}F nuclei, respectively. $I(Mn)$ and $I(^{19}F)$ are nuclear spin operators of the ^{55}Mn and ^{19}F (I = 1/2, 100% abundance) nuclei. Although calculated spectrum agrees well with the experimental results. Simulation of EPR of Mn^{2+} ion with S = 5/2 gave more complicated EPR spectra which were not detected in the experiment. Mn^{2+} ion in low-spin state exists in many compounds such as calcite and complex cyanides [23], pyrite structure compounds [24], Al_2O_3 [25], etc. Lower intensity lines between sextet bands could be attributed to forbidden transition in Mn^{2+} [25]. In this paper, the simulation of forbidden transitions is not performed due to complications in spin-hamiltonian constructing and low intensity and spectral resolution of forbidden transition related lines.

On the both sides of the spectrum strong broad EPR signal appears. It has a weak dependence on the sample orientation. These bands cannot be attributed to Ce^{3+} ion signal due to no EPR signal from the Ce^{3+} ion was observed in any sample at room and 77 K temperatures [23,26]. However, this signal could be attributed to some kind of radiation-induced centers, i.e. O^- centres that are the results of the exposure to natural radiation in the earth. The similar signal was assigned to O^- centres in [27,28]. The following study of origin of these bands is required.

4. Conclusion

In the present work, for the first time, a detailed chemical, crystal structural and physical study of agrellite specimen from the Dara-i-Pioz massif is carried out by means of EPMA, FTIR, EPR and SCXRD. The results are compared with new data obtained for agrellite from the Murun massif.

The simplified formula of the investigated agrellite samples is $NaCa_2[Si_4O_{10}]F$. REEs and Sr are present in the structure in very small quantities (≤0.04 apfu). Consequently, it is impossible to rank the Dara-i-Pioz and Murun agrellite as one of the previously described varieties: REE-agrellite [1,2] or Sr-agrellite [3–5]. SCXRD data show that the structural and chemical features of the studied samples are similar, but different with respect to ones of the Murun agrellite of previously described in [4]. Crystal structure of investigated samples corresponds to the model proposed for REE-agrellite [2].

For Dara-i-Pioz and Murun agrellites a structure of IR absorption band in Si-O vibration region is the same. Narrow absorption peak of OH is observed in the both samples. In H_2O/OH vibration region the spectra are different. In the sample from Murun massif the strong absorption band of H_2O molecule is present, but in Dara-i-Pioz sample no H_2O absorption is found.

In the both samples EPR signal attributed to Mn^{2+} ions is detected. HF and SHF splitting is the same. It is found out that manganese ion is normally substitutionally incorporated into agrellite crystal strucutre at Ca sites, surrounded by two fluorine ions.

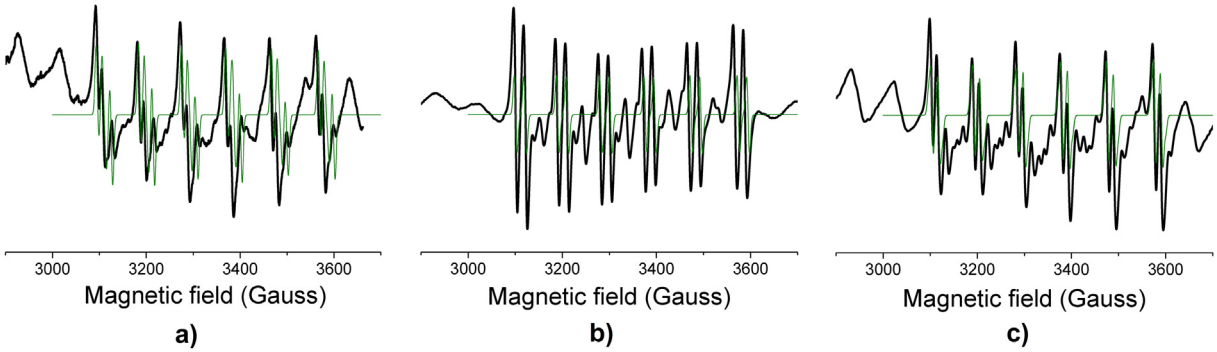

Fig. 5. EPR spectra of agrellite at 77 K: (a) **B** || [0 0 1]; (b) **B** || ⟨0 1 0⟩; (c) **B** ⊥ ⟨0 1 0⟩.

Luminescence due to 5d–4f transition in Ce^{3+} ions was observed in investigated samples. Band gap of agrellite was estimated at about 8 eV. Using VRBE model positon of trivalent and divalent lanthanide 4f states and Ce^{4+} charge transfer energy are estimated. Wide absorption band peaked at about 390 nm corresponds to the charge transfer transition of Ce^{4+}.

As a result of spectroscopic and structural data analysis, it can be concluded that materials based on agrellite doped with rare earth ions can be considered as promising phosphors. A minor amounts of Fe, Mn, Ce, Mg and Ba in the Dara-i-Pioz agrellite and Sr, Mn, Fe, Ce and Mg in the Murun samples, most likely, are located in [8]-coordinated Ca(1A) and maybe Ca(2B) positions. The main physical properties of the studied compound with a tubular structure depend not on the structural unit forming the tube (SiO-radical), but on the chemical composition of the polyhedral "walls" connecting them to each other.

Declaration of Competing Interest

The authors declare that they have no known competing financial interests or personal relationships that could have appeared to influence the work reported in this paper.

Acknowledgements

The authors thank Prof. Stefano Poli (University of Milan) for the facilities at the Electron Microprobe Laboratory at the Dipartimento di Scienze della Terra "Ardito Desio", Universita' degli Studi di Milano. The authors are grateful to P. Dorenbos for providing a package for evaluating the positions of lanthanide levels in band gap (VRBE generator for Origin). The study was performed using the equipment at the Center for Collective Use ("Center for isotopic-geochemical investigations" at Vinogradov Institute of Geochemistry SB RAS.

This work was supported by the grant of the President of the Russian Federation MK-936.2019.5. Experiments on thermal dihydroxylation were supported by grant of Russian Science Foundation RSF 18-72-10085.

Appendix A. Supplementary material

Supplementary data to this article can be found online at https://doi.org/10.1016/j.cplett.2019.136868.

References

[1] J. Gittins, M.G. Bown, D. Sturman, Agrellite, a new rock-forming mineral in regionally metamorphosed agpaitic alkalic rocks, Can. Min. 14 (1976) 120–126.
[2] S. Ghose, C.N. Wan, Agrellite, Na(Ca, RE)$_2$Si$_4$O$_{10}$F: a layer structure with silicate tubes, Am. Min. 64 (1979) (1979) 563–572.
[3] I.V. Rozhdestvenskaya, L.V. Nikishova, K.A. Lazebnik, Diagnostics of the agrellite polytypes using X-ray powder diffraction data, Proc. Russ. Min. Soc. 127 (1998) 89–94.
[4] I.V. Rozhdestvenskaya, L.V. Nikishova, Crystal structure of Na(Ca, Sr$_1$2Si$_O$4$_{O1}$0F strontium agrellite from Yakutian charoitites: agrellite polytypes, Crystallogr. Rep. 43 (1998) 589–597.
[5] A.A. Konev, E.I. Vorob'ev, A.N. Sapozhnikov, L.F. Paradina, I.L. Lapides, Z.F. Uschapovskaya, Strontium-containing agrellite from the region of the alkali Murun massif, Mineral. Jour. 9 (1987) 73–79.
[6] Bruker, APEX2, Bruker AXS Inc., Madison, Wisconsin, USA, 2003.
[7] Bruker, SAINT, Bruker AXS Inc., Madison, Wisconsin, USA, 2007.
[8] Bruker, SADABS, Bruker AXS Inc., Madison, Wisconsin, USA, 2009.
[9] P.W. Betteridge, J.R. Carruthers, R.I. Cooper, K. Prout, D.J. Watkin, Crystals version 12: software for guided crystal structure analysis, J. Appl. Cryst. 36 (2003) 1487, https://doi.org/10.1107/S0021889803021800.
[10] L. Palatinus, G. Chapuis, SUPERFLIP – a computer program for the solution of crystal structures by charge flipping in arbitrary dimensions, J. Appl. Cryst. 40 (2007) 786–790, https://doi.org/10.1107/S0021889807029238.
[11] D. Sofich, Yu.L. Tushinova, R. Shendrik, B.G. Bazarov, S.G. Dorzhieva, O.D. Chimitova, J.G. Bazarova, Optical spectroscopy of molybdates with composition $Ln_2Zr_3(MoO_4)_9$ (Ln: Eu, Tb), Opt. Mater. 81 (2018) 71–77, https://doi.org/10.1016/j.optmat.2018.05.028.
[12] F. Libeau, Structural Chemistry of Silicates: Structure, Bonding and Classification, Springer-Verlag, Berlin, Heidelberg, New York, Tokyo, 1985.
[13] E.V. Kaneva, N.V. Vladykin, E. Mesto, M. Lacalamita, F. Scordari, E. Schingaro, Refinement of the crystal structure of vlasovite from Burpala massif (Russia), Crystallogr. Rep. 63 (2018) 1092–1098, https://doi.org/10.1134/S1063774518070106.
[14] I.V. Rozhdestvenskaya, L.V. Nikishova, Crystallochemical characteristics of alkali calcium silicates from charoitites, Crystallogr. Rep. 47 (2002) 545–554, https://doi.org/10.1134/1.1496051.
[15] J.P. Perdew, A. Ruzsinszky, G.I. Csonka, O.A. Vydrov, G.E. Scuseria, L.A. Constantin, X. Zhou, K. Burke, Restoring the density-gradient expansion for exchange in solids and surfaces, Phys. Rev. Lett. 100 (2008) 136406, https://doi.org/10.1103/PhysRevLett. 100.136406.
[16] G. Socrates, Infrared and Raman Characteristic Group Frequencies: Tables and Charts, John Wiley & Sons Ltd., 2001.
[17] N.V. Chukanov, Infrared Spectra of Mineral Species: Extended Library, Springer Geochemistry/Minaralogy, Springer Science + Business Media, Dordrecht, 2014 10.1007/978-94-007-7128-4_1.
[18] R. Yu. Shendrik, I.I. Kovalev, A.I. Rusakov, V. Yu, Sokol'nikova, A.A. Shalaev, Luminescence of BaBr I crystal doped with Ce^{3+} ions, Phys. Solid State. 61 (2019) 830–834, https://doi.org/10.1134/S1063783419050329.
[19] R. Shendrik, A.A. Shalaev, A.S. Myasnikova, A. Bogdanov, E. Kaneva, A. Rusakov, A. Vasilkovskyi, Optical and structural properties of Eu^{2+} doped BaBr I and BaClI crystals, J. Lumin. 192 (2017) 653–660, https://doi.org/10.1016/j.jlumin.2017.07.059.
[20] P. Dorenbos, A review on how lanthanide impurity levels change with chemistry and structure of inorganic compounds, ECS J. Solid State Sci. Technol. 2 (2013) R3001–R3011.
[21] P. Dorenbos, Charge transfer bands in optical materials and related defect level location, Opt. Mater. 69 (2017) 8–22, https://doi.org/10.1016/j.optmat.2017.03.061.
[22] S. Stoll, A. Schweiger, EasySpin, a comprehensive software package for spectral simulation and analysis in EPR, J. Magn. Reson. 178 (2006) 42–55, https://doi.org/10.1016/j.jmr.2005.08.013.
[23] A. Abragam, B. Bleaney, Electron Paramagnetic Resonance of Transition Ions, Clarendon Press, Oxford, 1970.
[24] Y. Jiang-Tsu, H. Ying-Sheng, L. Shoei-Sheng, Electron paramagnetic resonance of low-spin Mn^{2+} in RuS_2 and $RuSe_2$, J. Phys.: Condens. Matter. 2 (1990) 5587–5594.
[25] V.J. Folen, "Forbidden" transitions in the paramagnetic resonance of Mn^{++} in Al_2O_3, Phys. Rev. 125 (1962) 1581, https://doi.org/10.1103/PhysRev. 125.1581.
[26] S.K. Mirsa, S. Isber, EPR of the Kramers ions Er^{3+}, Nd^{3+}, Yb^{3+} and Ce^{3+} in Y $(NO_3)_3{\cdot}6H_2O$ and $Y_2(SO_4)_3{\cdot}8H_2O$ single crystals: study of hyperfine transitions, Phys. B: Condens. Matter. 253 (1–2) (1998) 111–122, https://doi.org/10.1016/s0921-4526(98)00373-1.
[27] E. Abi-Aad, A. Bennani, J.-P. Bonnelle, A. Aboukaïs, Transition-metal ion dimers formed in CeO_2: an EPR study, J. Chem Soc, Faraday Trans. 91 (1995) 99–104, https://doi.org/10.1039/FT9959100099.
[28] M. Kumar, R.M. Kadam, T.K. Seshagiri, V. Natarajan, A.G. Page, TSL and EPR studies of $SrBPO_5$ doped with CeO_2 and co-doped with CeO_2 and Sm_2O_3, J. Radioanal. Nucl. Chem. 262 (3) (2004) 633–637, https://doi.org/10.1007/s10967-004-0486-7.